

Experiment and analysis of an optical measurement of spin-flip lifetimes of donor-bound electrons of n-GaAs



A thesis submitted towards partial fulfilment of
BS-MS Dual Degree Programme

by

URVASHI GUPTA

under the guidance of

PROF. DR. IR. CASPAR H. VAN DER WAL



PHYSICS OF NANODEVICES,
ZERNIKE INSTITUTE FOR ADVANCED MATERIALS,
UNIVERSITY OF GRONINGEN, THE NETHERLANDS



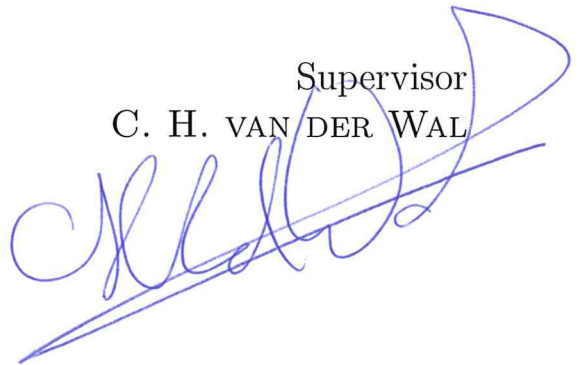
INDIAN INSTITUTE OF SCIENCE EDUCATION AND
RESEARCH, PUNE

Certificate

This is to certify that this thesis entitled "EXPERIMENT AND ANALYSIS OF AN OPTICAL MEASUREMENT OF SPIN-FLIP LIFETIMES OF DONOR-BOUND ELECTRONS IN n-GaAs" submitted towards the partial fulfilment of the BS-MS dual degree programme at the Indian Institute of Science Education and Research, Pune represents original research carried out by "Ms. URVASHI GUPTA" at "ZERNIKE INSTITUTE FOR ADVANCED MATERIALS, UNIVERSITY OF GRONINGEN, THE NETHERLANDS", under the supervision of "Prof. dr. ir. CASPAR VAN DER WAL" during the academic year 2014-2015.

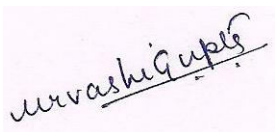
Student
URVASHI GUPTA

Supervisor
C. H. VAN DER WAL



Declaration

I hereby declare that the matter embodied in the report entitled "EXPERIMENT AND ANALYSIS OF AN OPTICAL MEASUREMENT OF SPIN-FLIP LIFETIMES OF DONOR-BOUND ELECTRONS IN n-GaAs" are the results of the investigations carried out by me at the "ZERNIKE INSTITUTE FOR ADVANCED MATERIALS, UNIVERSITY OF GRONINGEN, THE NETHERLANDS", under the supervision of "Prof. dr. ir. CASPAR VAN DER WAL" and the same has not been submitted elsewhere for any other degree.

A handwritten signature in black ink on a light pink background. The signature reads "Urvashi Gupta" in a cursive script.

Signature of the Student

URVASHI GUPTA

Date

25 March 2015

Acknowledgements

I would like to thank my supervisor Prof. Caspar van der Wal for giving me the opportunity to perform my Master's research under his guidance. I would like to express my gratitude to my supervisors Jakko de Jong and Danny O'shea for guiding me throughout my research. Without their daily guidance and immense help in the GaAs lab, I would not have been able to accomplish this work. I would like to specially thank them for their unconditional support and belief in my capabilities. I wish Danny a speedy recovery and hope he returns to lab soon. A special thanks to Xu for coming to my rescue during alignment problems and weekend filling sessions, to Olger for the short time I spent in the SiC lab and to all members of the QD team from whom I learnt a lot during the weekly meetings and physics discussions.

I would like to thank everyone at FND(Physics of Nanodevices group) for hosting me specially Prof. Bart van Wees and Prof. Tamallika Banerjee. It was a great experience to work and interact with so many enthusiastic physicists and learn more about their work. A special thanks to Martijn, Harman and Johan who came to our rescue each time we faced technical problems. I would also like to thank Sebastian, Xu, Jing, Geert and Arijit for a fun-filled work environment in the Masters' student room.

I would like to thank University of Groningen(Rug) for being my host and my institute IISER, Pune for allowing me to pursue my final year research as an exchange student at Rug. A special thanks to the Erasmus Mundus NAMASTE India-EU mobility scholarship that gave me this opportunity and brought me to Groningen. This city has given me my first experience abroad and it has been a truly memorable one.

Last but not the least, I would like to thank my parents for their endless support, guidance and love and my friends at both IISER and Groningen who have constantly inspired me to strive for my goals.

Abstract

Implementation of quantum communication requires material media that can store and process information. Recent studies have predicted that at low doping levels ($\leq 10^{14} \text{cm}^{-3}$) and low temperatures ($\leq 10\text{K}$) semiconductors have long coherence times and are promising candidates for studying quantum information processing. Experimental research work has also found the spin-flip lifetime (T_1) of n-GaAs to be of the order of a millisecond and has indicated the dependence of T_1 on the optical pumping field. In this work, we perform preparatory experiments with an ensemble of lambda systems formed by donor-bound electrons in n-GaAs using a polarization maintaining confocal microscope setup in a He-bath cryostat. We describe in detail, the procedure for finding a homogeneous ensemble in a sample of GaAs:Si. This work aims towards an optical measurement and the characterization of the spin-flip lifetime of the donor-bound electrons, to determine the dependence on optical pumping parameters. We further describe a Fabry-Perot filter cavity that has been designed for the detection of weak Raman photons during the experiment. The design of the cavity has been modified and its performance has been improved and characterized for the purpose of this experiment.

Contents

1	Introduction	3
2	D⁰-D⁰X lambda system in GaAs:Si	5
2.1	Neutral donors (D ⁰) and donor-bound excitons (D ⁰ X)	5
2.2	The lambda system	5
2.3	Polarization selectivity of optical transitions in the D ⁰ -D ⁰ X lambda system	6
2.4	The sample of n-GaAs	6
3	Motivation	7
3.1	Literature study	7
3.2	Experimental scheme	7
4	Experimental setup	10
4.1	Optical setup with a cryostat	10
4.2	A monolithic filter cavity for filtering of Raman signal photons	11
4.2.1	Motivation	11
4.2.2	Initial design and properties	12
4.2.3	Suppression	13
5	Results	16
5.1	Measurements on the Fabry-Perot filter cavity	16
5.1.1	Temperature response	16
5.1.2	Long term stability	17
5.2	Measurements on the sample of n-GaAs	20
5.2.1	Finding the sample	20
5.2.2	Finding a good spot on the sample	20
5.3	Identifying D ⁰ -D ⁰ X transitions	22
6	Summary and future prospects	24

Chapter 1

Introduction

Advancements in technology have led to the miniaturization of electronic devices. As a result, processing powers of classical computers have tremendously improved helping us solve many of the mysteries of nature. However, as we progress to much smaller scales, quantum phenomena become significant and must be taken into account. Certain complex problems such as the factorization of large numbers that are extremely difficult to solve classically, could be solved using quantum computing tools. The laws of quantum mechanics combined with cryptography thus form the basis of quantum information science. The ideas of quantum superposition and entanglement can then ensure faster and highly secure means of quantum communication.

To achieve the aim of long distance quantum communication, there arises a need for a medium for propagation of information. Photon states come across as promising candidates for carrying quantum information. They ensure speedy and secure communication as they move with the speed of light and interact weakly with the environment. The spin states of electrons in semiconductors which optically couple well with photons are promising candidates for storage of quantum information. Such material media whose spin states can then extract quantum information from carrier photons and can store and process this information must have long coherence times to be used as quantum memory. So far the concept of quantum memory has been studied extensively in non-solid state environments such as single atom or ion traps [1, 2]. These systems address a single qubit and are very useful for initial insights and research. However, implementation of such systems for large scale technological applications is difficult. Semiconductors on the other hand, provide scope for implementing micron-sized devices that can be fitted into optical fibers for advanced applications [3]. Moreover, working with ensembles allows us to address many atoms collectively rather than a single atom. When addressed in the right geometry, ensembles give a directional optical response that is highly detectable in the presence of a strong excitation background [4, 5].

III-V semiconductors, in particular GaAs have been studied for decades and can be grown in a very controlled manner to obtain a clean sample with a homogeneous ensemble. Moreover, they have been found to have long coherence times. Though the nuclear spins in these semiconductors limit their coherence times, these are long enough for studying the fundamental physics of quantum memory in solid-state spin ensembles. We have thus chosen to work with n-type GaAs.

Two important parameters characterize the coherence of a system - the spin relaxation time (T_1) and the decoherence time (T_2). T_1 is the time taken by an electron to align itself with an applied external magnetic field. T_2 , on the other hand is the time taken

by electrons precessing about an external magnetic field (applied perpendicular to the spin direction) to lose their relative phase information. While T_2 is extremely difficult to measure, it is possible to measure the inhomogeneous decoherence time, also known as the dephasing time (T_2^*). T_2^* has been measured for various materials and has been found to be broadly in the range of picoseconds to microseconds. However, fundamentally it is the T_1 that limits T_2 . Thus, an estimate of T_1 can give us further insight into the coherence properties of materials that can become efficient media for quantum optics and quantum communication. Previous theoretical work [6, 7] has indicated that T_1 for n-GaAs quantum dots is long and of the order of milliseconds. Long spin-flip lifetimes in GaAs quantum dots have also been demonstrated in experimental work by Colton *et al* [8]. In bulk n-GaAs, this has been demonstrated experimentally by Kai Mei C. Fu *et al* [9] where they measure T_1 in the lambda systems of donor-bound electrons in n-GaAs to be of the order of a millisecond when the system is allowed to evolve in the dark. While the spin relaxation times are often assumed to be constant parameters of a system, a careful observation of the work [9] gives an indication that T_1 changes when the optical pumping field is on. Our aim is to investigate this dependence of T_1 in the lambda system of donor-bound electrons of n-GaAs on laser illumination. In this experiment, we not only want to study the effect of illumination on T_1 while resonantly addressing the transitions of the lambda system but also would like to investigate its influence when the lasers are detuned or even off-resonant from any known transitions.

In this work, we perform preparatory experiments towards measurement and characterization of T_1 in our sample of n-GaAs. We want to measure T_1 by probing the optical transitions between Zeeman sublevels in lambda systems of donor-bound electrons of n-GaAs and detecting Raman scattered photons that signify spin-flip in reflection and transmission. For this, we first designed, characterized and improved the working of a temperature controlled Fabry-Perot filter cavity which will be used to filter and distinguish the weak Raman photon signals of our measurements from the strong background laser light. We then look for a spot on our sample with characteristic absorptive features that correspond to the excited states in the lambda systems of donor-bound electrons. Once we have located such a spot, we characterize the optical transitions of donor-bound electrons at high magnetic fields by performing transmission spectroscopy. Upon locating each of the transitions of the lambda system, we can perform measurements to estimate T_1 and ultimately study its behavior with the laser parameters.

Outline of the thesis

In this thesis, we describe the preparatory work done towards the spin-flip lifetime measurement of donor-bound electrons in n-type GaAs. Chapter 2 introduces the reader to a brief (theoretical) description of lambda systems formed by donor-bound electrons in n-GaAs and the optical transitions that we address in our experiments. In chapter 3, we give a detailed literature study of T_1 measurements with GaAs and its dependence on illumination. We elaborate on the experimental scheme we choose to follow and our motivation for carrying out this work. Chapter 4 describes the experimental setup and the filter cavity designed for our experiments. Chapter 5 is devoted to characterization and results of our measurements on the filter cavity and our sample. Finally, in chapter 6 we conclude and describe the next steps towards the main aim of our research.

Chapter 2

D^0 - D^0X lambda system in GaAs:Si

In this chapter, we describe the D^0 - D^0X lambda systems formed by silicon donors in a gallium arsenide lattice.

2.1 Neutral donors (D^0) and donor-bound excitons (D^0X)

The silicon(Si) dopants in GaAs are electron donors when at Ga sites. They donate the extra electrons to the conduction band. However, at temperatures below the ionization temperature of donors ($\leq 10K$), these electrons remain bound to the Si donor atoms. Further, for doping $\leq 10^{14} \text{ cm}^{-3}$, the Si atoms are far apart such that the wave functions of the bound electrons do not overlap. The Si donor atoms thus form an ensemble of non-interacting hydrogen-like systems (called the neutral donor D^0).

The Donor-bound exciton complex (D^0X) consists of an exciton X (a weakly bound electron and hole pair) bound to the neutral donor D^0 by Coulomb attraction. It is a trion consisting of two electrons in the spin-singlet state and one hole.

Each of the donor atoms in the D^0 - D^0X systems has a similar environment and the same wave function. Hence, the transitions associated with these systems have narrow linewidths and low inhomogeneity which makes them promising systems for experimental work towards quantum information processing.

2.2 The lambda system

In absence of an external magnetic field, the 1s ground state of D^0 is doubly degenerate. When a magnetic field is applied, it splits into two states - the spin-up state $|\uparrow\rangle$ and the spin-down state $|\downarrow\rangle$ due to the Zeeman effect. At an applied field of $B = 7T$, these spin states are 35 GHz apart with the $|\uparrow\rangle$ at a lower energy. The two states are populated approximately in the ratio of 2:1 when in thermal equilibrium at liquid helium ($T=4.2K$) temperatures. The two Zeeman split states of D^0 form the two ground states and the lowest level of D^0X forms the excited state of the lambda system that we address in our experiments. A schematic diagram of the D^0 - D^0X lambda system is shown in Figure 2.1.

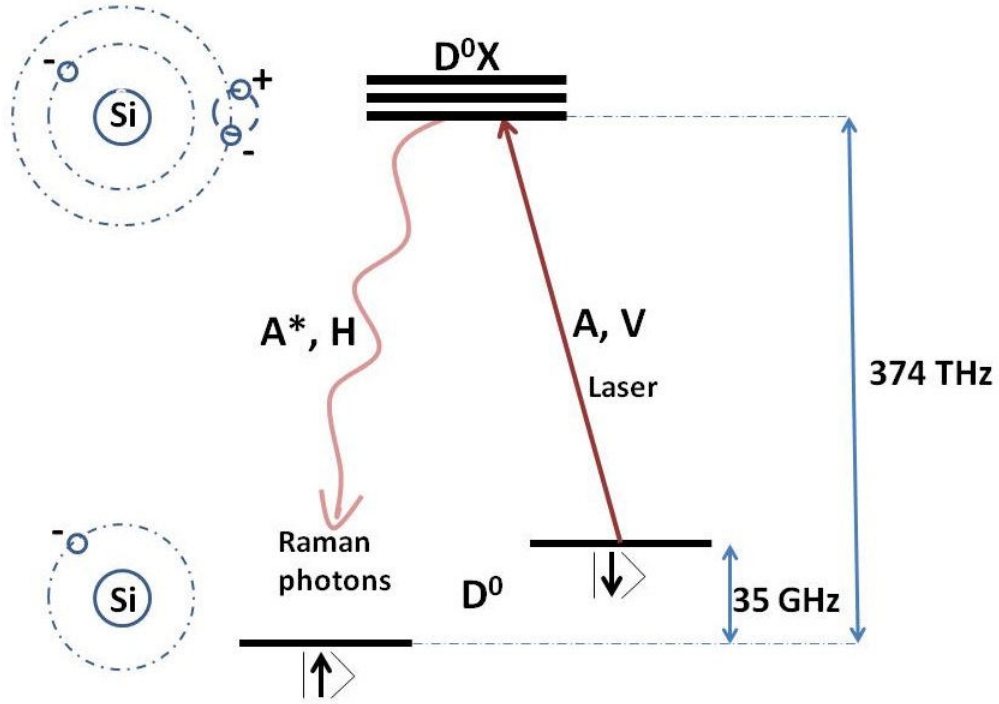


Figure 2.1: The D^0 - D^0X lambda system

2.3 Polarization selectivity of optical transitions in the D^0 - D^0X lambda system

When a magnetic field is applied orthogonal to the direction of propagation of light, the transitions of the D^0 - D^0X lambda system can be addressed selectively using two orthogonal linear polarizations of light. The transition from the $|\downarrow\rangle$ state to the excited state $|e\rangle$ is denoted as the A transition and is selective to horizontally polarized light. The other transition from the $|\uparrow\rangle$ state to the $|e\rangle$ state is denoted as the A^* transition and is selective to vertically polarized light.

2.4 The sample of n-GaAs

The film of GaAs:Si that we use was grown epitaxially with low Si doping at a donor concentration of 10^{14} cm^{-3} . They were transferred to a sapphire substrate by an epitaxial lift-off technique and fixed there by van der Waals forces. The thickness of the GaAs film is $10 \mu\text{m}$.

Chapter 3

Motivation

We performed a literature study of the work done on T_1 measurements with GaAs. In the following section, we present some of the studies that have inspired us to further investigate the spin relaxation time and its dependence on laser illumination.

3.1 Literature study

Two interesting theoretical studies have been performed for electrons in n-GaAs quantum dots. In the study done by Khaetskii *et al* [6], a number of spin-orbit mechanisms have been studied and spin-flip lifetimes of longer than microseconds have been predicted. Further, Woods *et al* [7] suggest spin-phonon coupling mechanisms that contribute to the long spin-flip lifetimes in n-GaAs quantum dots. While relaxation mechanisms in quantum dots are significantly different, similar studies done for bulk semiconductors have indicated that relaxation arises from spin-orbit coupling mediated by phonon or impurity scattering [7, 10, 11].

An experimental study done by Colton *et al* [8] has reported spin-flip lifetimes for lightly-doped ($3 \times 10^{15} \text{ cm}^{-3}$) bulk n-GaAs. They used circularly polarized light to initialize the spins and probed them with photo-luminescence after different resting times. The degree of circular polarization of emitted light was proportional to the spin polarization of the sample. The spin-flip lifetimes for bulk n-GaAs were reported to be $1.4 \mu\text{s}$ which agrees with theoretical predictions [6].

Another experimental study has been performed by Kai-Mei C. Fu *et al* [9] for measurement of the spin-flip lifetime (T_1) of donor-bound electrons in low doped bulk n-GaAs. This research work has measured T_1 to be of the order of milliseconds which is the longest reported value so far. Further, there is an indication of dependence of T_1 on laser parameters which we elaborate in the next section and forms the basis for our motivation to measure and characterize T_1 in donor-bound electrons of n-GaAs.

3.2 Experimental scheme

In order to measure and verify T_1 , we will be closely following the experimental scheme used by Fu *et al* [9]. A schematic picture of the steps involved in T_1 measurement has been shown in the Figure 3.1

The basic scheme of the experiment involves applying a long pulse on the A transition such that all the population from the $|\downarrow\rangle$ state is optically pumped to the $|\uparrow\rangle$ state.

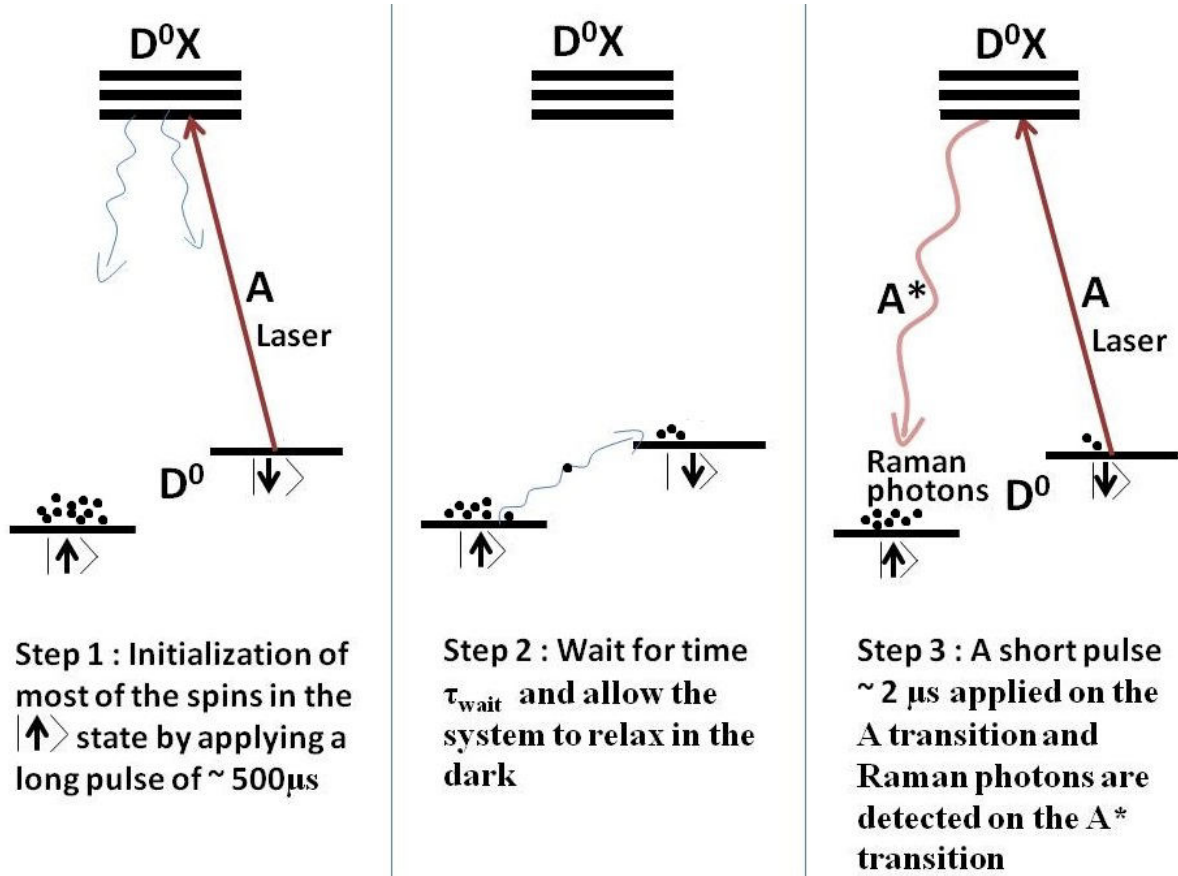


Figure 3.1: Experimental scheme adopted by Kai-Mei Fu *et al* [9]

For a sufficiently long pulse of about $500\mu\text{s}$, we can safely assume that most of the population has been pumped into the other state. Using an acousto-optic modulator, the laser beam is deflected and the system is allowed to evolve in the dark for a time τ_{wait} . After this, a pulse of about $2\mu\text{s}$ is applied on the A transition again and emission of Raman photons on the A^* transition is detected. The detected number of counts n should now be proportional to the population that has relaxed back to the $|\downarrow\rangle$ state during the waiting time τ_{wait} .

These steps are repeated for different waiting times and the number of counts is plotted for each τ_{wait} as shown in the Figure 3.2. The τ_{wait} for which the curve levels off to

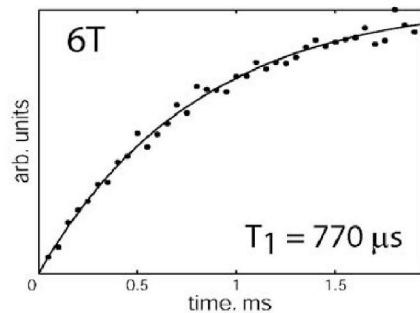


Figure 3.2: Plot of no. of photon counts detected on A^* transition for different values of τ_{wait} [9]

its thermal equilibrium value is calculated using the exponential fit equation 3.1 for

population relaxation. This is the characteristic spin-flip lifetime (T_1) of the electrons in the D^0 - D^0X lambda system. A T_1 of $770 \mu s$ has been measured from the plot above. The longest reported spin-flip lifetime in this experiment was of the order of milliseconds which is also the longest reported so far for n-GaAs.

$$n = n_{eq}(1 - e^{\tau/T_1}) \quad (3.1)$$

Fu *et al*[9] show the applied programmed pulse and some typical data obtained from time-resolved photo-luminescence of the A^* transition in the Figure 3.3. The high number of

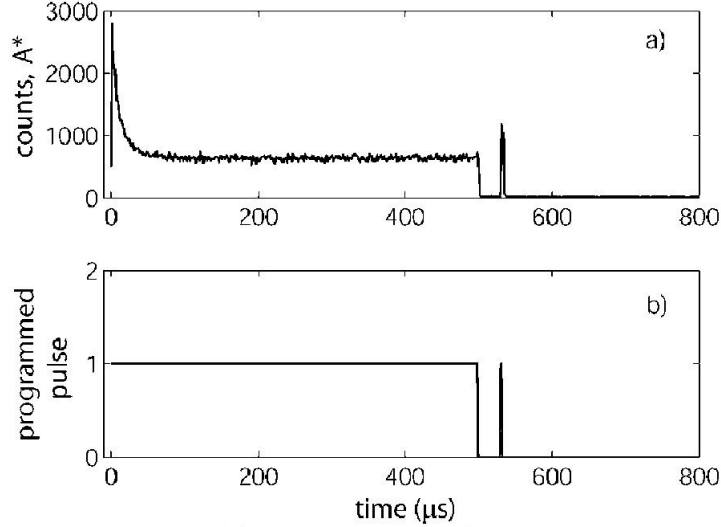


Figure 3.3: An example of the programmed pulse and the corresponding counts detected [9]

photon counts on the A^* transition in the first $20 \mu s$ indicate optical pumping between the Zeeman sub-levels. However, a closer look reveals that after about $30 \mu s$, the plot levels off to a non-zero number of counts which means that the population has been partially recovered. The ratio of recovered population to the pumped population was expected to be zero because D^0X is known to have nanoseconds relaxation times and the spin relaxation time (T_1) are expected to be greater than $100 \mu s$. This is a strong indication that T_1 depends on laser illumination and must be shorter when the optical pumping field is on.

The main objective of our experiment is to investigate the dependence of spin relaxation on laser illumination and how T_1 depends on the optical pumping field parameters such as laser power, frequency and detuning. Such a characterization can give us an insight about how the coherence times of a system can be manipulated and improved for applications to quantum information processing and quantum communication.

Chapter 4

Experimental setup

In this chapter, we first describe the fiber-based confocal microscope of the optical setup in the cryostat that we will use for experiments on the GaAs sample. This setup is based on the one designed by Sladkov *et al*[12] but has some important modifications. Later, we elaborately discuss characterization and improvement of a monolithic Fabry-Perot filter cavity that we will need for detection of Raman photons in the T_1 experiment.

4.1 Optical setup with a cryostat

The sapphire plate carrying the thin film sample of GaAs:Si is placed on a Γ -shaped copper holder. The sample holder is mounted on a three axes (xyz) stack of piezomotors (Attocube ANPx101, ANPy101, ANPz101). This entire setup is mounted in a dipstick that is lowered into a sealed vacuum chamber inside a closed He-bath cryostat. A superconducting magnet provides magnetic fields upto 9 T in the z (vertical) direction.

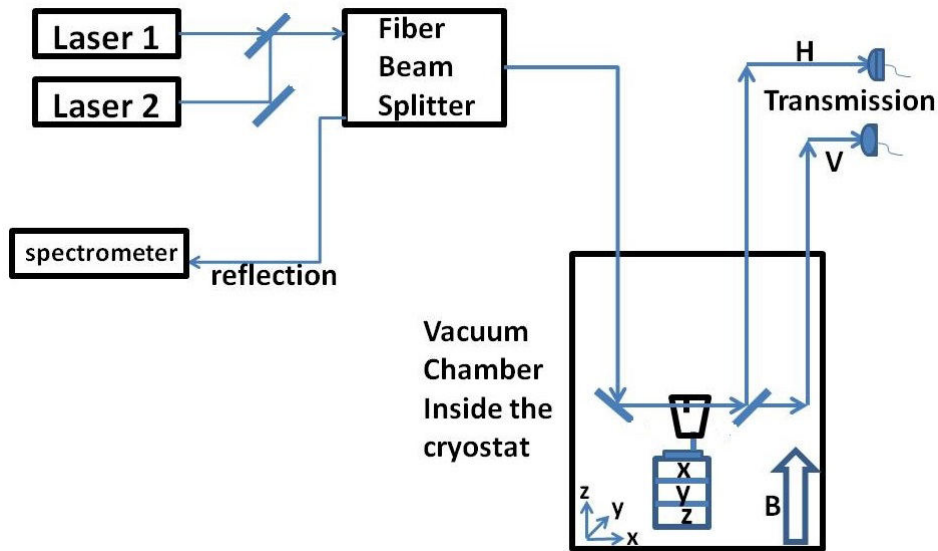


Figure 4.1: A schematic diagram of the experimental setup for T_1 measurements

The optical setup for our experiments includes two tunable continuous-wave Ti:sapphire lasers (Coherent MBR-110) and a diode laser (Newfocus velocity). Light from both the MBR lasers is coupled into a polarization maintaining optical fiber (PMF). The PMF

operates on the principle of linear birefringence such that two TEM modes can carry orthogonal linear polarizations and light in one mode does not couple to light in the other mode. The light from the fiber falls on a prism mirror that changes the direction of propagation by 90° . We thus work in the Voigt geometry ($\vec{k} \perp \vec{B}$) which allows us to address orthogonal linear polarization selectivity of the transitions of the D^0 - D^0X system. The light is then focused on the sample by two aspheric lenses that form a confocal microscope [12]. The reflected light from the sample and emitted light from the sample both retrace their optical path through the PMF back into the fiber beam splitter. This light can then be detected at the spectrometer. The transmitted light from the sample is split with a polarizing beam splitter (inside the chamber) into two orthogonal linear polarizations H and V which are coupled into two multimode fibers (non-polarization maintaining) that deliver the light outside the cryostat. The transmitted light from these fibers is detected using a photo-diode.

The closed cryostat does not provide free optical access to the sample. To find the sample and to move it into the focus of the microscope, a single laser is used. The laser frequency is set to a value higher than the bandgap of GaAs, where the sample is opaque. The sample can be brought into the focus of the objective by moving the x axis piezo-motors towards or away from the PMF that delivers the light onto the sample. The y and z piezo-motors are used to move the sample horizontally or vertically to position the sample in the path of the beam. The reflection and transmission signals can be monitored to position the sample in the beam path and at the focus of the microscope objective. We discuss this further and in detail in Section 5.2.1.

4.2 A monolithic filter cavity for filtering of Raman signal photons

4.2.1 Motivation

The T_1 experiment involves pumping the transitions between Zeeman split sub-levels of the ground state $|g\rangle$ and the excited trion state $|e\rangle$ in the lambda systems formed by the donor-bound electrons in n-GaAs. The energy difference between the two Zeeman split sub-levels $|\uparrow\rangle$ and $|\downarrow\rangle$ is small and only 35 GHz while the transitions from the sub-levels to the excited state $|e\rangle$ are at 374 THz. The final step of the T_1 measurement as shown in Figure 4.2 involves probing the A transition and detecting Raman scattered photons on the A^* transition or vice-versa.

The low probability of Raman scattering and emission of Raman photons in random directions results in low efficiency of collection of the signal photons. As a result, the power difference between these signal photons and the excitation light is of the order of 10^9 . To successfully detect these weak photons, there was a need to suppress the strong excitation background light by selective filtering. The resonance frequency of such a filter must be tunable to A or A^* transition and must have maximum suppression at the other transition 35 GHz away from the resonant mode. For this, the cavity must have a resulting full spectral range (FSR) of 70 GHz to obtain maximum suppression.

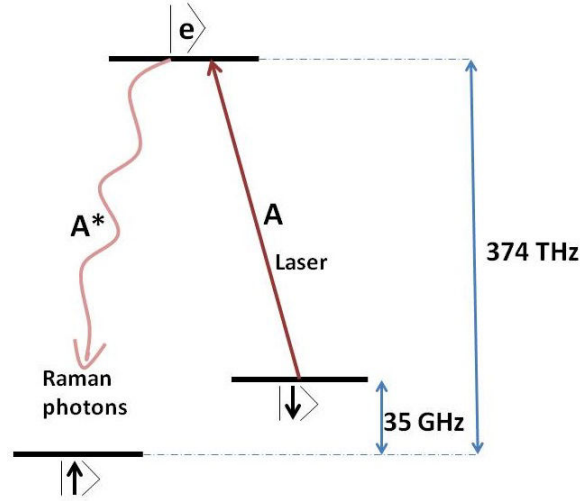


Figure 4.2: Lambda system of donor-bound electrons in n-GaAs

4.2.2 Initial design and properties

Inspired by the work of Palittapongarnpim *et al* [13], a filter cavity was designed by Carmem using the concept of a Fabry-Perot resonator [14]. While a regular etalon uses flat mirrors which are easy to align and also provide spectral filtering, curved mirrors ensure higher finesse and filtering of spatial modes in addition to the spectral filtering. In order to optimize all these factors, a plano-convex lens of radius of curvature 40.31mm with a highly reflective coating ($R = 99.0\% \pm 0.5\%$ for $\lambda = 815\text{-}825\text{nm}$) was chosen as a filter cavity. The cavity had a thickness of 1.5mm to obtain a full spectral range close to 70 GHz [14]. A transmission spectrum of the cavity aligned with the TEM_{00} mode is shown in Figure 4.3.

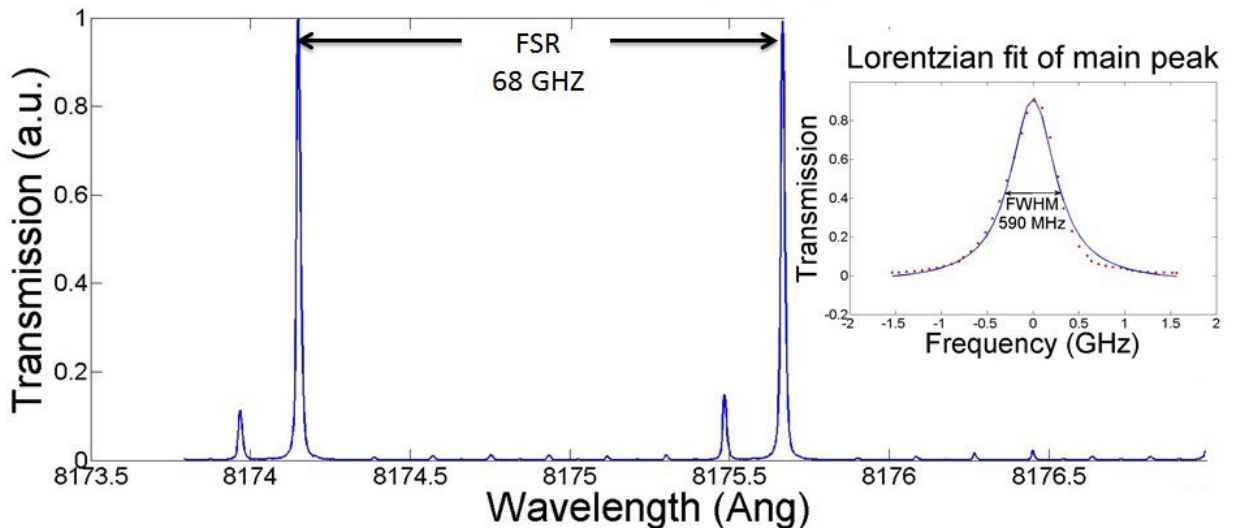


Figure 4.3: Summary of Carmem's result [14]

The effective finesse (\mathfrak{F}) of the cavity is limited by factors such as the reflectivity (R), presence of defects on the reflecting surfaces and alignment of beam and cavity axes [13].

It is thus difficult to achieve the ideal finesse of 300. Moreover, a narrow fundamental mode might end up losing most of the Raman photons to be detected. A fundamental mode-width of 400 MHz was thus chosen for this cavity [14]. For an FSR close to 70 GHz and a mode-width of 400 MHz, an effective finesse of 170 was calculated using the equation 4.1.

$$\mathfrak{F} = \frac{FSR}{\Delta\nu} \quad (4.1)$$

The mode-width was extracted from a lorentz fit of the fundamental mode of the transmission spectrum (Figure 4.3 :inset) and reported to be 590 MHz which was much broader than the required value of 400 MHz. The measured FSR of 68 GHz was reasonably close to the required value of 70 GHz. With this setup, the suppression achieved was of the order of 10^3 with a finesse of 115 [14].

For the purpose of the T_1 experiment, the cavity must remain locked to the laser for measurements recorded over few hours or even one or two days. This cavity was found to be stable for slightly less than two hours. In order to improve the performance of this cavity, important changes have been made to this design. The next three sections are devoted to the changes made to the cavity design and a comparative study of the characterization results with those of the initial design.

4.2.3 Suppression

Collimation of the beam and alignment of the beam axis with the cavity mode are the most critical factors to achieve the highest suppression of unwanted modes from the cavity [13]. The optical setup for alignment and mode matching is shown in Figure 4.4. To collimate the incoming beam, a Schäfter-Kirchhoff collimator was used with a

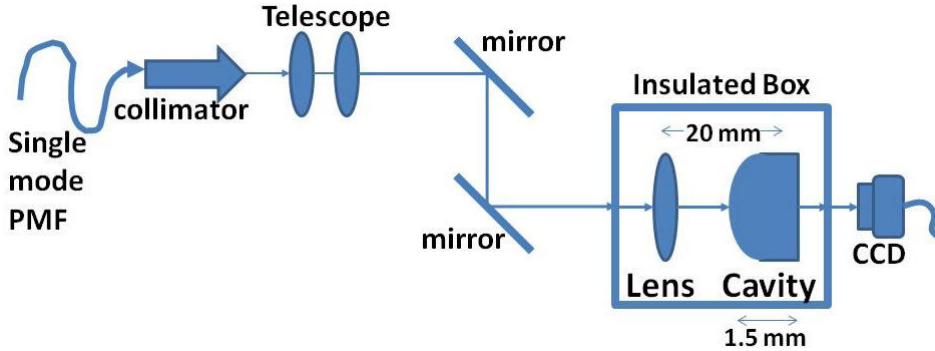


Figure 4.4: Optical Setup for alignment and mode matching

telescope in succession. The distance between the telescope lenses could be adjusted with a micrometer screw to have a beam spot size of $49\mu\text{m}$ calculated from the cavity parameters [14]. The collimated beam was focused onto the flat side of the cavity by the focusing lens of focal length 20mm placed in a lens cage with the cavity. Two mirrors were placed to adjust the position and angle of the beam falling on the cavity. After a rough manual alignment, the transmitted beam profile was observed with a CCD camera. If the incoming beam hits the cavity off-axis, it hits the cavity surface multiple times at different spots which form an ellipse of spots in the beam image (Figure 4.5 (a)). For a perfectly aligned cavity, the beam retraces its path inside the cavity resulting in the

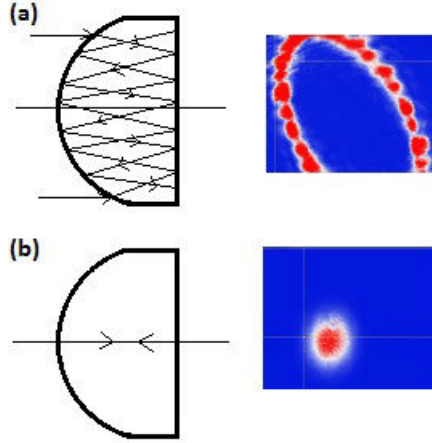


Figure 4.5: (a) Off-axis illumination (b) Axial illumination [14]

beam hitting exactly the same spot multiple times. The transmitted beam appears as a single spot on the camera as shown in Figure 4.5(b). The two mirrors are carefully tuned to match the beam axis with the cavity such that all the spots squeeze together into a single beam spot. This, however only roughly aligns the cavity as is seen in the cavity spectrum by replacing the camera with a photo-diode. We still observe some of the higher order spatial modes in the cavity spectrum. A maximum suppression of 1.5×10^3 was achieved which was an order of magnitude less than the expected value of 10^4 .

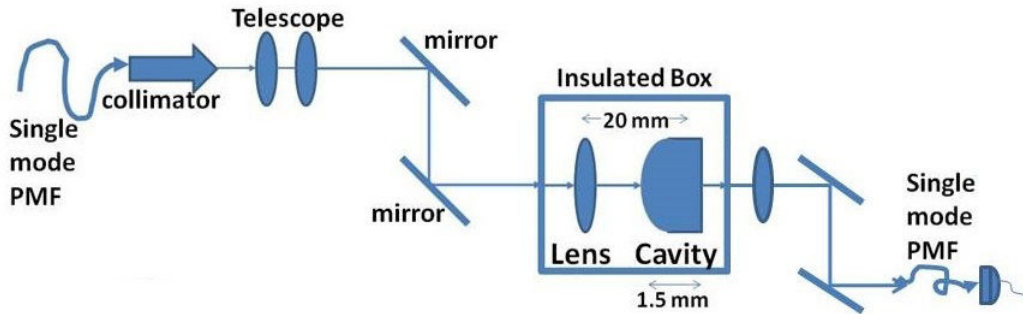


Figure 4.6: Improved setup with transmitted light coupled into a single mode optical fiber

For further improvement of the overall suppression such that the transmission spectrum is devoid of any higher order spatial modes, we used two mirrors after the cavity to couple the transmitted light into a single mode polarization maintaining optical fiber as shown in Figure 4.6. A transmission spectrum was recorded by modulating and scanning a diode laser over one FSR of about 2.5 \AA and detecting the coupled light at the other end of the fiber using a photo-diode connected to a lock-in amplifier to suppress the background noise.

The resulting spectrum (Figure 4.7) has higher transmission of the fundamental mode relative to the unwanted secondary mode. After coupling the light into the single mode optical fiber, most of the unwanted modes were suppressed. The maximum suppression has increased to 5.6×10^3 (Figure 4.8). In combination with the polarization filtering

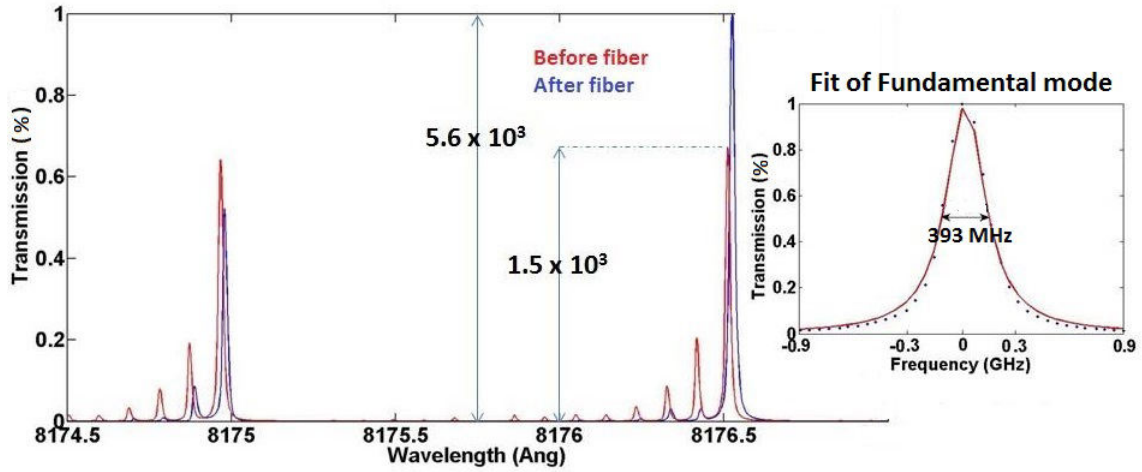


Figure 4.7: A comparative plot of transmission spectrum before and after coupling light into a single mode fiber

inside the cryostat (order 10^1) and the spectrometer (order 10^4), we can thus achieve a desired extinction of the order of 10^9 .

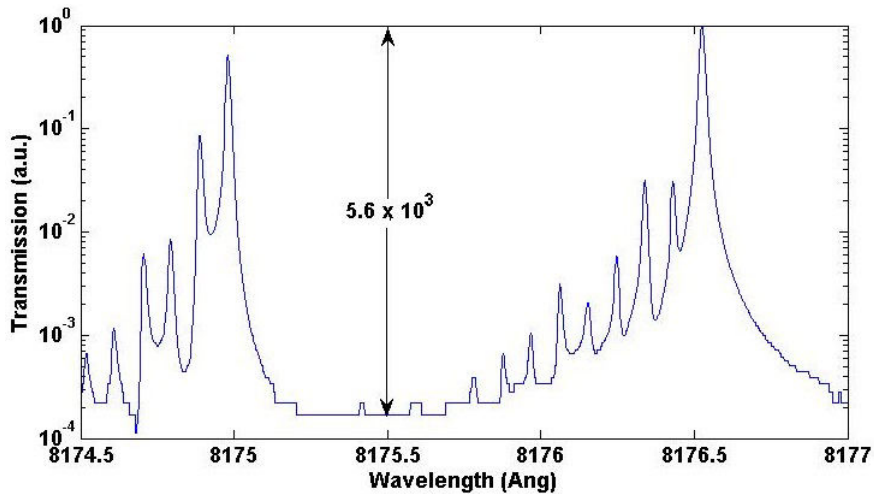


Figure 4.8: A Log-scale plot of transmission spectrum of the cavity

Further, the fundamental mode of this spectrum was fitted with a intensity profile equation derived for spherical resonators that resembles a Lorentzian as shown in the Figure 4.7 : inset. From the fit parameters, a mode-width($\Delta\nu$) = 393 MHz and finesse(\mathfrak{S}) of 176 was calculated for a free spectral range (FSR) of 69.2 GHz. In comparison to the fit parameters from the initial cavity design ($\Delta\nu = 590MHz$, $\mathfrak{S} = 115$, $FSR \approx 68GHz$), the cavity performance has significantly improved and agrees well with the expected values ($\Delta\nu = 400MHz$, $\mathfrak{S} = 170$, $FSR = 68GHz$).

Chapter 5

Results

5.1 Measurements on the Fabry-Perot filter cavity

5.1.1 Temperature response

The resonance frequency of the cavity depends on the cavity length and refractive index of the material which can be tuned with temperature [14]. Thus, by changing the temperature of the cavity the resonant mode of the cavity could be tuned to a desired frequency. Assuming a linear thermal expansion, the resonance frequency should linearly depend on the temperature as follows:

$$\frac{d\nu}{dT} = -\nu \left(\frac{1}{L} \frac{dL}{dT} + \frac{1}{n} \frac{dn}{dT} \right) \quad (5.1)$$

$$= -\nu \left(\alpha + \frac{1}{n} \frac{dn}{dT} \right) \quad (5.2)$$

Here ν is the resonance frequency, n is the refractive index, α is the thermal expansion coefficient and T is the temperature of the cavity.

In order to achieve this temperature tunability, a temperature feedback system was put together as shown in Figure 5.1 to monitor and change the temperature of the cavity. A peltier element (Thorlabs part TEC3-2.5) and a thermistor (TH10K) were used in combination with a proportional integrated differential temperature controller box (TEC200C). The lens cage carrying the focusing lens and the cavity was mounted on the cool side of the peltier which is placed with its hot side on the aluminium box that acts as the heat sink. The thermistor is placed near the cavity and not too far from the peltier to sense the temperature of the cavity accurately. Thermal grease was used to coat all the contact areas for good thermal contact and accurate detection of temperature.

With this setup, the temperature of the cavity was tuned to different values in the range 15°C to 25°C and a transmission spectrum was recorded for each value of temperature. The drift in resonance frequency of the fundamental mode (TEM₀₀) was calculated and plotted with the temperature. The temperature response of the cavity was reported to be 1.21 GHz/°C [14]. This was significantly lower than the expected temperature response of 3.14 GHz/°C that was calculated using theoretically documented values of thermal expansion coefficient and dn/dT for BK7 material from literature [15, 16]. A temperature tunability of 1.21 GHz/°C meant that a temperature range of 58°C would enable us to tune the cavity over one complete FSR.

To further improve the temperature response of the cavity, it was necessary to eliminate

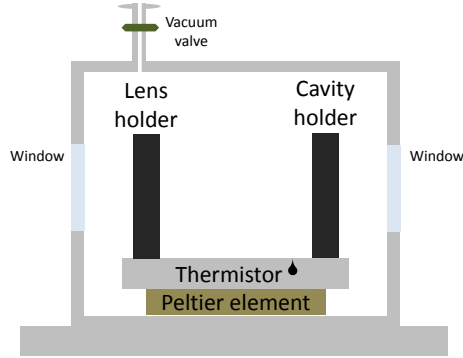


Figure 5.1: Temperature feedback and cage setup in the initial design [14]

any thermal leaks that cause the temperature of the cavity to be unstable. The air from the aluminium box was pumped down to a pressure of 10^{-5} mbar thus thermally isolating the cavity from the surroundings.

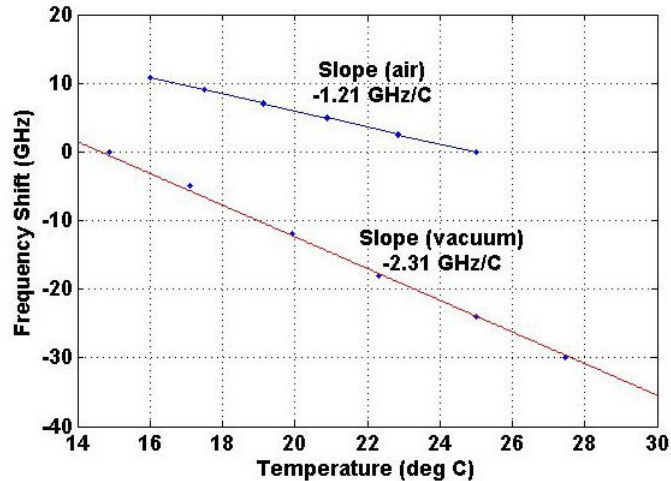


Figure 5.2: Temperature response obtained after evacuating the box

The transmission spectra were recorded for different temperatures in the same way as before. The plot of drift of resonance frequency vs temperature (Figure 5.2) shows that the temperature tunability achieved is $2.308 \text{ GHz}/^\circ\text{C}$. Thus, by thermally isolating the cavity from the environment, the temperature response has almost doubled such that we can now span the entire spectral range within a temperature range of 30°C .

5.1.2 Long term stability

For the purpose of our experiments towards measurement of T_1 , we need the filter cavity to function with high stability for over a few hours or even over a day. This implies that the resonance frequency of the cavity must be more or less stable at a set value of temperature with minimum drift away from the corresponding frequency. A high stability is characterized by a root-mean-square drift of less than 10% of the full width at half maximum (FWHM) of the transmission peak. The plot of the resonance frequency shift with time in Figure 5.3 shows that the cavity is stable for about 2 hours with this design. A frequency drift of just 4% of the linewidth [14] is observed.

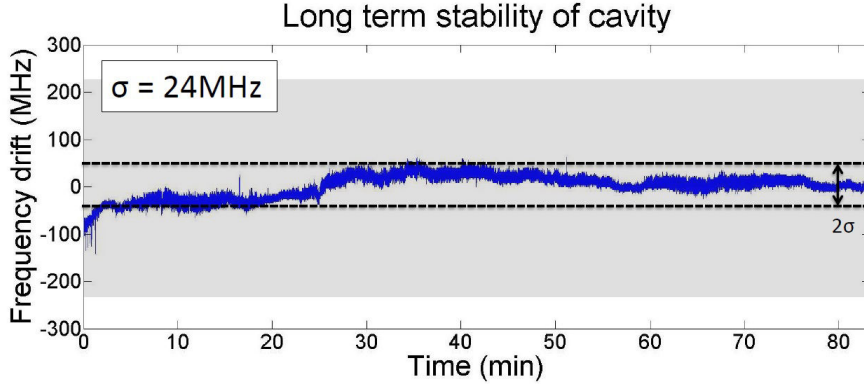


Figure 5.3: Plot of resonance shift with time. Gray shaded area is the linewidth of the transmission peak and the dotted line shows the root-mean-squared of the drift. [14]

To measure the long term stability of the cavity, an MBR-110 laser (stabilized within 15 MHz) is locked to the frequency at which we obtain about 40% of the maximum of the transmission peak. At this point, the relation between the frequency drift and transmission voltage is approximately linear. The temperature of the cavity is kept stable within 0.005°C using a PID system of the temperature controller box. The voltage is detected by a photo-diode and recorded every minute using a lock-in and voltage-meter for several hours.

For a profile resembling a Lorentzian, a Taylor approximation reveals that a shift in frequency at half the maximum transmission is linearly dependent on the change in the transmission (Figure 5.4). Thus, a drift in the recorded voltage with time translates into the resonance drift directly as follows:

$$\Delta\nu = FWHM(T - T_0) \quad (5.3)$$

Here, $\Delta\nu$ is the frequency shift, FWHM is the full width at half maximum of the transmission peak and T_0 is the average transmission.

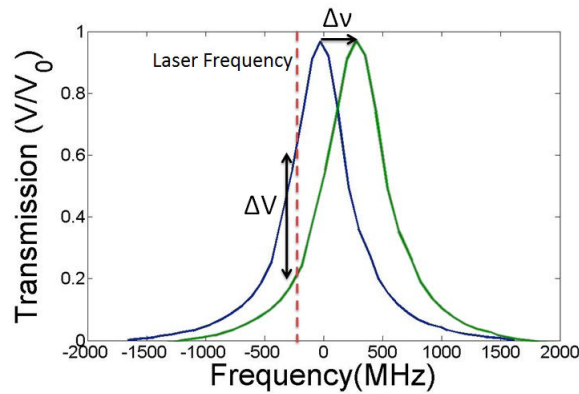


Figure 5.4: Relation between the frequency drift and voltage drift [14]

We repeated this measurement after introducing vacuum in our setup and observed that the cavity is reasonably stable for over seven hours as shown in the Figure 5.5. The root-mean-squared drift is 31.6 MHz which is 8% of the linewidth of the transmission peak which is 393 MHz.

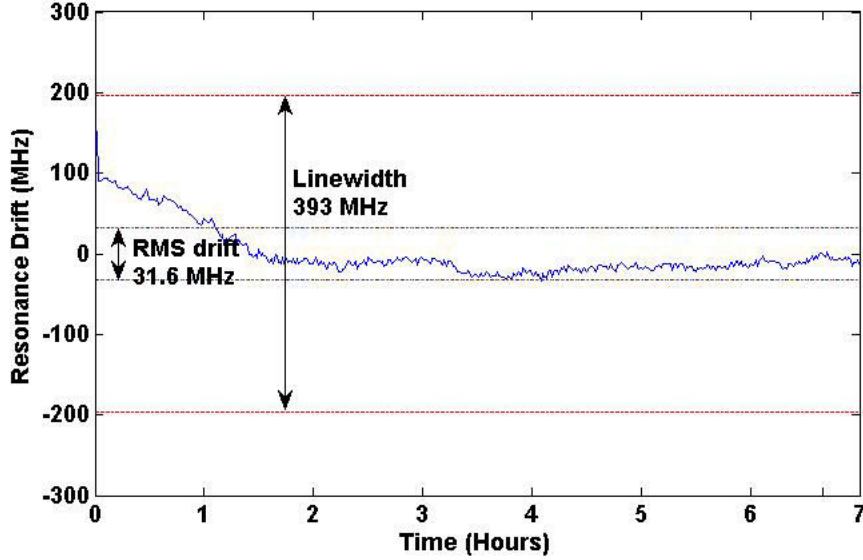


Figure 5.5: Long term stability plot after evacuating the box

Though the cavity is reasonably stable, some measurements show that the stability is variable and uncertain. This could be attributed to the use of metallic screws to mount the cavity on the aluminium base of the box. The use of long wires for electric connections of thermistor and peltier element to the temperature controller adapter attached to the box roof could be the cause of resistive heating which creates significant temperature drifts inside the box resulting in drifts in the resonance frequency of the cavity. We thus decided to replace the metallic screws with plastic ones and reduce the lengths of the connecting wires as much as possible. The design of the cavity has been modified to achieve this and is shown in the Figure 5.6.

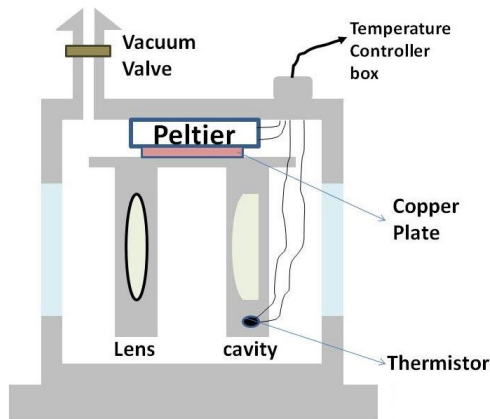


Figure 5.6: Modified design of the filter cavity box

We now want to test the long term stability of this new design. If stable for a long time, we can characterize its parameters again as shown in the preceding sections. The Fabry-Perot cavity will then be ready to use for our experiment for filtering Raman photons and measuring T_1 .

5.2 Measurements on the sample of n-GaAs

In order to perform successful experiments, we have to find a suitable spot on the sample where we can clearly identify donor-bound exciton systems. Such a spot must show clear D^0X absorptions and can be identified with some distinct features which are elaborately discussed in section 5.2.2. Since, we don't have direct optical access to the sample in the cryostat, we need to first find the sample and bring it in the focus of the microscope objective so that we get maximum intensity in reflection and transmission from the sample. We describe the procedure for finding the sample and bringing it in focus in the following section.

5.2.1 Finding the sample

To find the sample, we fix the MBR laser frequency to a value in the bandgap of GaAs where the sample is opaque and monitor the reflection and transmission signals with a photo-diode connected to a lock-in amplifier and a voltage-meter.

Upon cooling the sample to liquid nitrogen (77 K) and later to liquid helium temperature (4.2 K), the focal point of the confocal microscope may change slightly. The best way is to have the sample in focus in air before the dipstick carrying the sample is lowered into the cryostat and cooled down to low temperatures. The first step is to make sure that the sample is in the central position by moving the y and z piezo-motors and observing the sample with the naked eye. Having the sample approximately in the center means that it is in the optical path of the beam. Then we use the x piezo-motor to move the sample to different positions towards or away from the fiber scanning laterally along the y axis (width of the sample). If the sample is in focus, we should see a sharp peak in the reflection signal and a sharp dip in the transmission signal. At this point, it is best not to move the x piezo-motor any further to avoid moving the sample out of focus.

During cool down, each of the piezo-motors is moved a small distance in both direction to make sure that the piezo-motors do not freeze at such low temperatures due to moisture between the moving parts. After the dipstick is loaded into the cryostat, one must immediately change the voltage of the piezo-motors to the documented value for liquid nitrogen and liquid helium temperature. The temperature of the dipstick can be determined by looking at the capacitance of the piezo-motors. We continue moving the piezo-motors slightly in both directions until the capacitance of the piezo-motors comes down to the respective documented values. Minor adjustments of the x piezo-motor then bring the sample back into focus. These steps should be repeated after cooling the sample to liquid nitrogen temperature and then again cooling it down to liquid helium temperature.

5.2.2 Finding a good spot on the sample

The next major and challenging step towards T_1 measurement is the characterization of the D^0 system in the sample of n-GaAs. For this, we need to find a spot on the sample where we can identify and address the transitions of the D^0 system clearly. We keep the sample in focus and move around the sample using the y and z piezo-motors only.

In the Figure 5.7, we show single laser scans at a bad spot and a suitable spot on the sample. The first feature that one must look for is a broad, regular and highly pronounced Fabry-Perot background at wavelengths in the range 8170-8180 Å which is slightly higher

than the bandgap. Such a background is an indication of low inhomogeneous broadening. This is followed by a free exciton absorption of about 2.5 \AA broad at around 8182 \AA wavelength. One must look for a spot with a narrower and sharper absorption against the pronounced Fabry-Perot background. This too is an indication of homogeneity in the sample. The next major indication is another narrow and pronounced Fabry-Perot background at wavelengths following the free exciton absorption. At higher wavelength, we see another narrow absorption that corresponds to D^0X but is not as deep as the free exciton. This is normally followed by two consecutive absorption dips about 0.4 \AA apart corresponding to zero-field splitting observed in the D^0X levels.

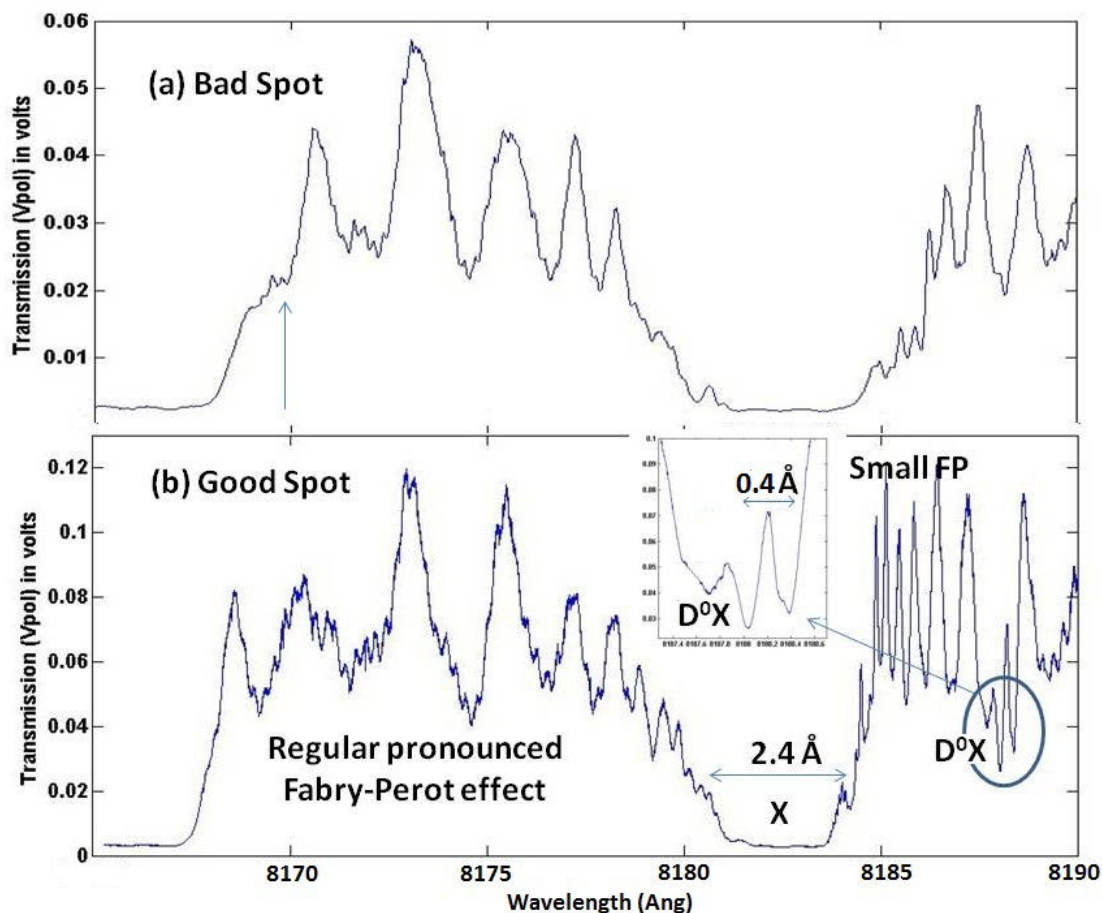


Figure 5.7: Example of a bad spot and a suitable spot for experiments on the sample

For a good spot, each of these absorptive features must be sharper, narrower and more pronounced. The entire pattern must be shifted to lower wavelengths (blue-shifted) or higher energies with highly pronounced Fabry-Perot background. Moreover, it should not have any other random pronounced absorptive features that tend to hide the above mentioned characteristics that we are looking for. The pattern must look clean with these distinct features in both the transmission channels (H and V polarized light from the sample).

From past experience and experiments performed on this sample, we know that the probability of finding a suitable spot is higher on the left edge of the sample. The sample sticks to the sapphire plate better at the left edge leading to lesser strain than at other regions on the sample. We first lower the frequency of the piezo-motors so that the laser

scans the sample very slowly over the sample. We then record the transmission signal at different spots along one chosen direction (y or z). We chose to move to different spots along the z direction near the left edge and look for spots where transmission is high. We stop at a spot where the transmission is comparatively higher than the surrounding region. We take a single laser scan at this spot in the wavelength range of the D^0 - D^0X system using a chopper in the beam path and lock-in techniques. One way to look for a good Fabry-Perot background is to lock the MBR laser at the slope of the first Fabry-Perot pattern as shown by the upward arrow on the bad spot in Figure 5.7 (a). We then look for high transmission regions again moving stepwise in the vicinity of the current spot with the y or z piezo-motors and taking single laser scans with the diode laser for different spots and comparing them.

Once at a reasonably good spot, we can continue to move around it stepwise taking single laser scans and comparing them to fix the best available spot for all the further experiments. This is one of the most trying phases of the experiment. Once at a suitable spot, we can further perform pump-assisted transmission spectroscopy to characterize the polarization dependence of the D^0 - D^0X transitions at high magnetic field.

5.3 Identifying D^0 - D^0X transitions

We use pump-assisted transmission spectroscopy to identify A and A^* transitions of the D^0 - D^0X lambda system in n-GaAs. A schematic diagram of the lambda system is shown in Figure 5.8. As described in section 2.3, these transitions are polarization selective when addressed at high magnetic fields in the Voigt geometry.

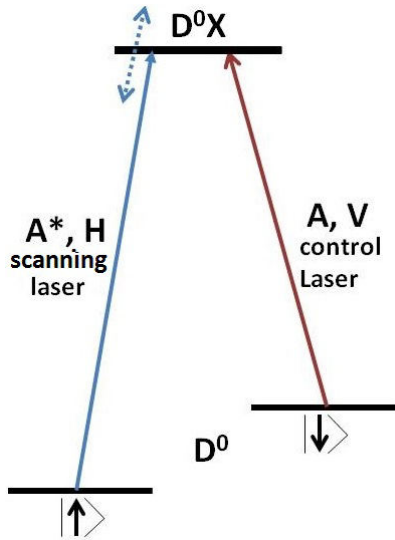


Figure 5.8: The D^0 - D^0X lambda system

The transmission spectra are recorded at 5.82T with the help of two lasers at the magnetic field. The pump laser (MBR) is locked at the wavelength corresponding to one of the transitions and optically pumps this transition. Meanwhile, the diode laser scans the other transition with two different polarizations - H and V . These two scans can be compared to identify transitions and characterize their polarization dependence. The pump laser is modulated with a chopper in the beam path using lock-in amplifiers. It is about 10 times stronger in power than the scanning laser and prevents population

depletion by the scanning laser.

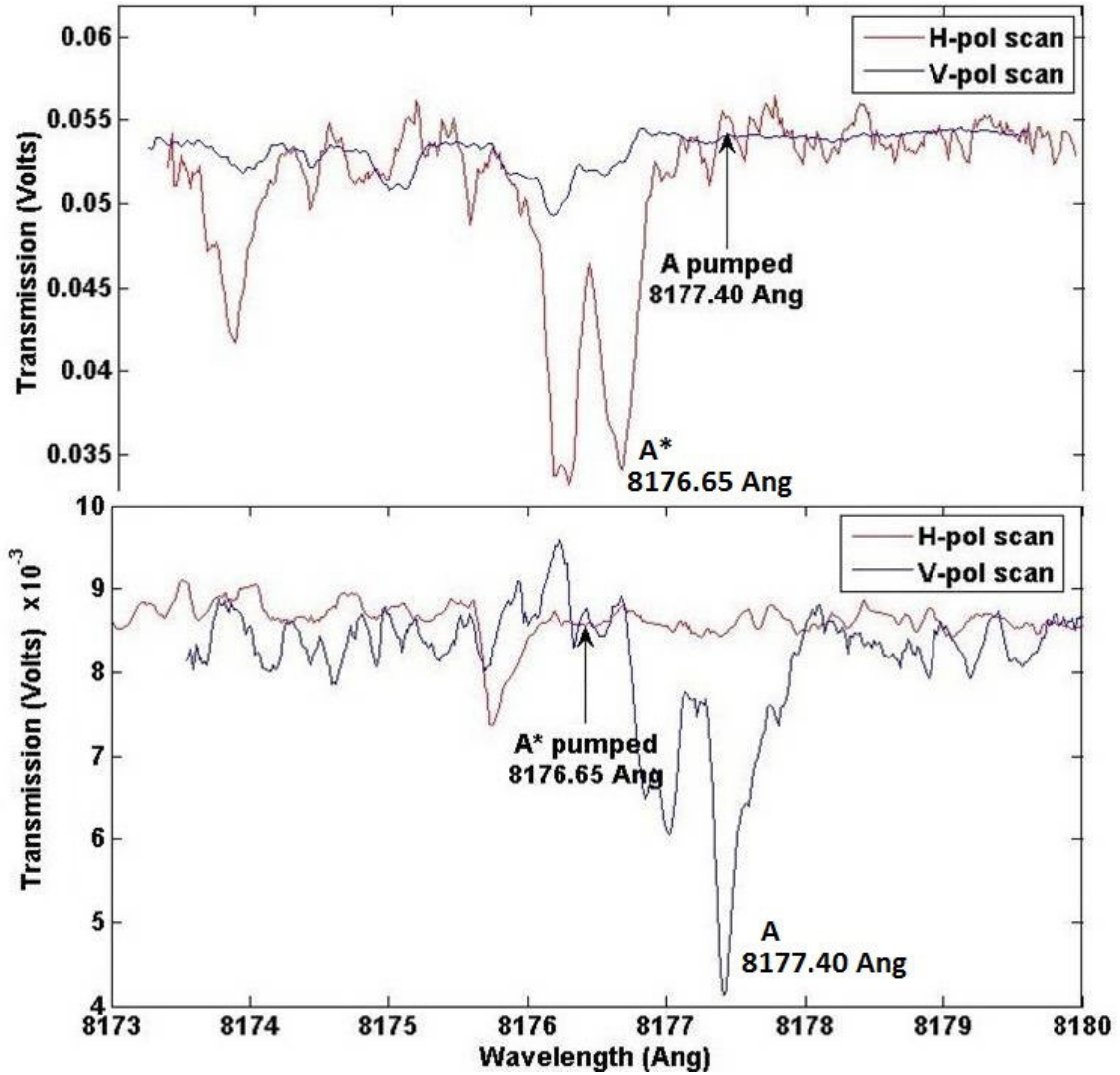


Figure 5.9: Pump-assisted spectroscopy to identify transitions with polarization selectivity

In the Figure 5.9, we show comparative spectra for the diode laser scanning the A* transition with H and V polarizations with the pump laser locked at the A transition (V-polarized) wavelength of 8177.4 Å. We observe that at around 8176.6 Å, the absorption is more enhanced in the H-polarized scan than in the V-polarized scan and thus corresponds to the A* transition. Similarly, when the pump laser is fixed at the A* transition (H-polarized) wavelength of 8176.6 Å and the diode laser scans the A transition with H and V polarizations, we see an enhanced absorption at the wavelength of 8177.4 Å for the V-polarized light but not with the H-polarized light.

Chapter 6

Summary and future prospects

In this thesis, we have described and demonstrated some experimental methods towards the measurement of spin-flip lifetimes of donor-bound electrons in n-GaAs. For quantum information processing (QIP) applications, there is a need for material media that have long coherence times. The lambda systems formed by donor-bound electrons and donor-bound excitons in GaAs:Si are promising candidates for quantum optics experiments towards QIP. These systems have been found to have long spin-flip lifetimes (T_1) of the order of milliseconds and long dephasing times (T_2^*) of the order of nanoseconds. Moreover, optical transitions in these systems when addressed at high magnetic fields in the Voigt geometry are polarization selective. Studying such systems can give us further insights into experiments towards implementation of long distance quantum communication.

We have elaborately discussed a technique for the measurement and characterization of the spin-flip lifetimes based on the results of Kai-Mei Fu *et al* [9]. An indication of the dependence of spin-flip lifetimes on laser illumination forms our motivation for this work. We have described why we expect the T_1 (which is often considered a constant parameter) to be a function of laser parameters such as frequency and detuning. We then describe some preparatory experiments performed towards a measurement of T_1 of donor-bound electrons in n-GaAs. These involve experiments that identify the donor-bound electron systems in n-GaAs and characterize the polarization selective transitions of the three-level lambda systems formed by these electrons by pump-assisted photoluminescence and spectroscopy techniques.

T_1 measurements with n-GaAs involve detection of Raman signal photons which are 10^9 times weaker and just 35 GHz apart from a strong background laser of 374 THz. For filtering these photons for detection, a temperature tunable filter cavity had been designed. A number of important changes have been made to the original design of the cavity and its functioning and response has been recharacterized. We have been able to highly improve the performance of the cavity. The temperature response of this cavity has doubled and a long term stability of over 7 hours has been achieved due to these changes. Since T_1 measurements require the cavity to be stable for longer durations, we are working towards achieving it with the new design described in this work.

With these steps we are ready for performing measurements on the sample of n-GaAs that will help us understand the effect of the optical pumping field on the spin-flip lifetimes of donor-bound electrons. We can then manipulate these parameters to further enhance the spin-flip times and hence the coherence times of GaAs. This material can be used as quantum memory media for other experiments towards the study of entanglement phenomena for quantum communication applications.

Bibliography

- [1] C. W. Chou, H. de Riedmatten, D. Felinto, S. V. Polyakov, S. J. van Enk and H. J. Kimble, *Measurement-induced entanglement for excitation stored in remote atomic ensembles*, Nature, **438**, 828 (2005).
- [2] D. N. Matsukevich, T. Chaneleliere, S. D. Jenkins, S. Y. Lan, T. A. Kennedy, *Entanglement of Remote Atomic Qubits*, Phys. Rev. Lett., **96**, 030405 (2006).
- [3] M. D. Lukin, A. Imamoglu, *Controlling photons using electromagnetically induced transparency*, Nature, **413**, 273 (2001).
- [4] L. M. Duan, M. D. Lukin, J. I. Cirac and P. Zoller, *Long-distance communication with atomic ensembles and linear optics*, Nature, **414**, 413 (2001).
- [5] C. H. van der Wal, M. D. Eisaman, A. André, R. L. Walsworth, D. F. Phillips, A. S. Zibrov and M. D. Lukin, *Atomic memory for correlated photon states*, Science (New York, N. Y.), **301**, 196 (2003).
- [6] A. V. Khaetskii and Y. V. Nazarov, *Spin-flip transitions between Zeeman sublevels in semiconductor quantum dots*, Physical Review B, **64**, 1253160 (2001).
- [7] L. M. Woods, T. L. Reinecke and Y. Lyanda-Geller *Spin relaxation in quantum dots*, Physical Review B, **66**, 161318(R) (2002).
- [8] J. S. Colton, T. A. Kennedy, A. S. Bracker, D. Gammon, *Microsecond spin-flip times in n-GaAs measured by time-resolved polarization of photoluminescence*, Physical Review B, **69**, 121307(R) (2004).
- [9] Kai-Mei C. Fu, Wenzheng Yeo, Susan Clark, Charles Santori, Colin Stanley, M. C. Holland, Yoshihisa Yamamoto *Millisecond spin-flip times of donor-bound electrons in GaAs*, Physical Review B, **74**, 121304(R) (2006).
- [10] F. Meier and B. P. Zakharchenya, *Optical Orientation*, Chapter 3, North-Holland, Amsterdam (1984).
- [11] E. L. Ivchenko and G. Pikus, *Superlattices and Other Microstructures*, Springer, Berline (1995).
- [12] M. Sladkov, M. P. Bakker, A. U. Chaubal, D. Reuter, A. D. Wieck and C. H. van der Wal, *Polarization-preserving confocal microscope for optical experiments in a dilution refrigerator with high magnetic field*, Review of scientific instruments, **82**, 043105 (2011).

- [13] Pantita Palittapongarnpim, Andrew MacRae and A. I. Lvovsky, *Note: A monolithic filter cavity for experiments in quantum optics*, Review of Scientific Instruments, **83** , 066101 (2012)
- [14] Carmem M. Gilardoni, Danny O'Shea and C. H. van der Wal, *Characterization of a monolithic Fabry-Perot cavity for near-resonance Raman photon detection*, Bachelor Research Thesis, Physics of Nanodevices, University of Groningen (2014).
- [15] Volume Precision Glass Inc., www.vpglass.com/optical_glass/bk7_glass.html, online accessed October 9 (2014).
- [16] Schott Catalogue, *Optical Glass 2014, Description of Properties*, online accessed October 9 (2014).